Characterizing the Water Vapor Profiling Measurements at the ARM SGP CART Site

D. D. Turner
Pacific Northwest National Laboratory
Richland, Washington

W. F. Feltz
University of Wisconsin
Madison, Wisconsin

W. L. Smith
National Aeronautics and Space Administration
Langley Research Center
Hampton, Virginia

Introduction

The U.S. Department of Energy's Atmospheric Radiation Measurement (ARM) Program has helped facilitate the development of two advanced methods of profiling water vapor in the lower atmosphere at its Southern Great Plains (SGP) Cloud and Radiation Testbed (CART) site. Accurate, high spatial and temporal resolution profiles of water vapor are required for many endeavors, including assimilation into mesoscale models to improve nowcasts/forecasts, characterization of the atmospheric state for radiative transfer research, and transport and cloud processes research. These two methods complement the traditional in situ profiles of water vapor by radiosondes.

The two techniques are not new, but have been developed with the support of the ARM Program to operational status. One technique is a passive retrieval of water vapor and temperature profiles from a fully automated ground-based infrared interferometer called the Atmospheric Emitted Radiance Interferometer (AERI). The AERI provides high-resolution downwelling radiance spectra at better than 1 wavenumber resolution from 3.3-μm to 18-μm every 8 minutes. Careful attention to calibration results in absolute calibration accuracy better than 1% ambient radiance (Revercomb et al. 1993). From these spectra, temperature and moisture profiles are retrieved by inverting the radiative transfer equation using an iterative technique (Feltz et al. 1998; Smith et al. 1999). By using temperature and water vapor profiles retrieved from the Geostationary Operational Environmental Satellites (GOES) brightness temperature data (Menzel et al. 1998), together with the AERI's ground-based radiance information, detailed tropospheric profiles can be retrieved under clear and broken sky conditions. The vertical resolution of this combined data product is 100 meters in the lowest kilometer, and slowly degrades to 1 km resolution at 8 km. There are five AERI instruments located in the SGP CART domain, each of which is currently retrieving profiles of temperature and water vapor operationally.

The second profiling technique is an active remote sensor. A 24-hour operational Raman Lidar was developed as part of ARM's instrument development program and is stationed at the SGP central facility (Goldsmith et al. 1998). This system was designed to operate unattended, requiring only brief attention during startup and periodic cleaning of the enclosure's window. While Raman Lidars have shown tremendous water vapor profiling capability during the nighttime for some time (Melfi et al. 1989, for example), the daytime solar background hampers the detection of the weak Raman scattered signal. This lidar uses dual field-of-view and narrowband interference filters to block out the large solar background during the day, which enables the lidar to profile throughout the diurnal cycle. The maximum temporal resolution of this system is one minute, with a maximum of 39-meter vertical resolution. However, to improve the signal-to-noise, averaging in time and space is done, and a basic data product having 10-minute temporal resolution and 78-m vertical resolution is produced.

The Raman Lidar requires a single, height-independent scale factor to provide calibrated profiles of water vapor mixing ratio. Traditionally, radiosondes have been used to provide this constant. However, the ARM Program, as well as other researchers, has demonstrated that the sondes exhibit a large sonde-to-sonde variability in calibration, especially between calibration batches. However, the 2-channel Microwave Radiometer (MWR) located at the central facility, which retrieves total precipitable water vapor in the column overhead, has proven to be a very stable. Thus, the calibration factor needed by the Raman Lidar is derived from the MWR (Turner and Goldsmith 1999).

This paper provides results from an approximate 8-month period from April to December 1998. During this period, the Raman Lidar was operational approximately 60% of the time, collecting almost 22,000 10-minute profiles. The majority of the downtime was due to power bumps at the SGP site, which triggered the laser interlock and shut down the system. (The system requires clear skies to align itself during the initial startup; cloudy or inclement weather situations could delay startup for a period of hours to days.) Over the same period, the retrieval algorithm running on the AERI at the central facility, located within 200 m of the Raman Lidar, converged and retrieved over 33,000 profiles, which is about 75% of the total possible. Radiosondes are routinely launched by ARM at the central facility (the launch site is approximately 100 m from both the lidar and the AERI), and during this period about 1,000 launches occurred. An example of coincident profiles from each of these systems is given in Figure 1.

The high-resolution measurements from the AERI and Raman Lidar allow a better description of the thermodynamic state of the atmosphere than radiosondes, especially when the water vapor field is changing rapidly. For example, Figure 2 shows a dryline that passed over the CART site on April 13, 1998, which was observed by all three measurement systems. The two radiosondes launched this day at 11:30 Universal Time Coordinates (UTC) and 23:30 UTC were unable to capture the structure of the passage. However, the structure captured by active and passive remote sensors show remarkable agreement.

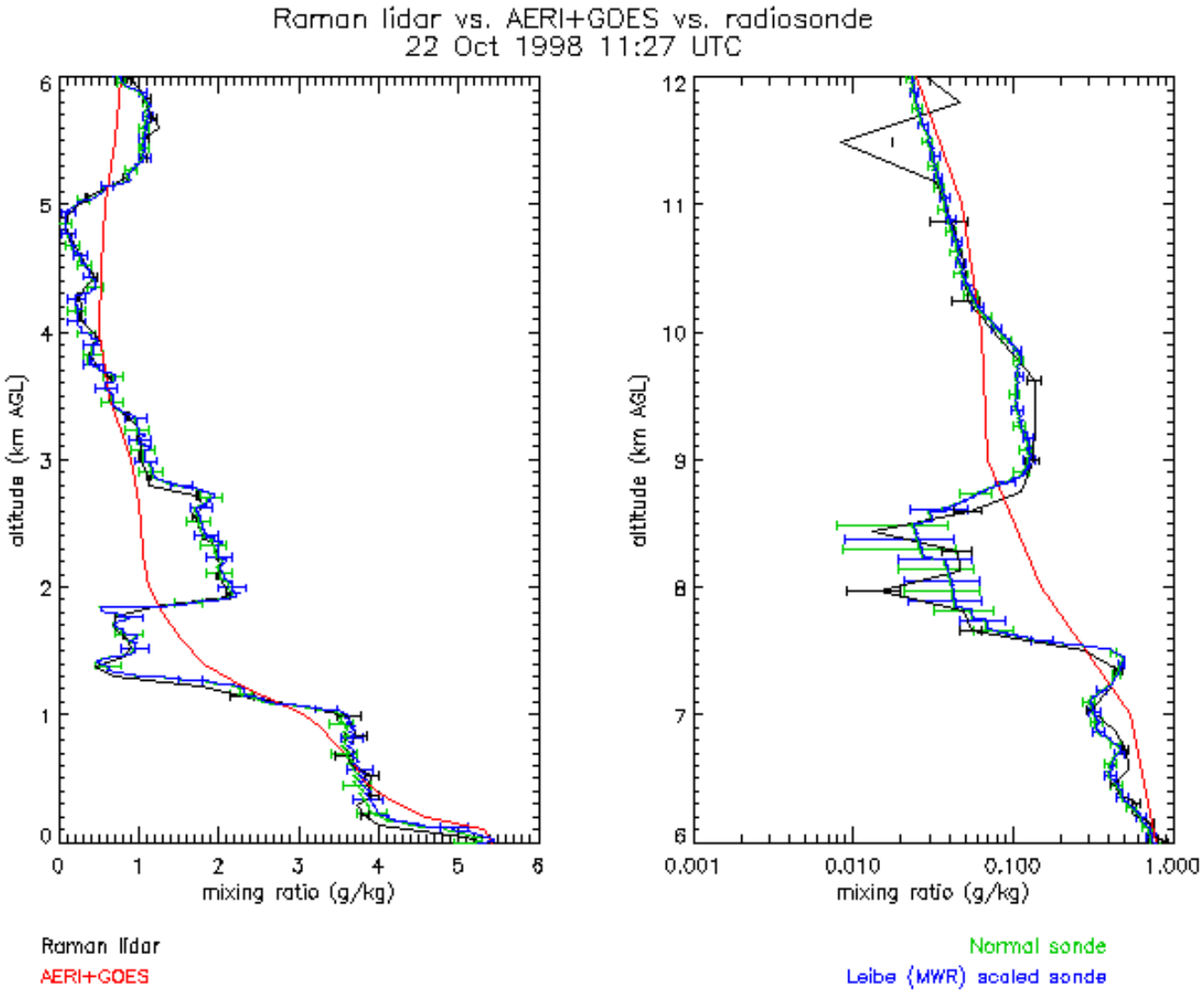

Figure 1. Example profiles of mixing ratio from the Raman Lidar (black) with error bars, normal (green) and MWR scaled (blue) radiosondes with error bars, and AERI retrievals (red) for October 22, 1998, at 11:27 UTC.

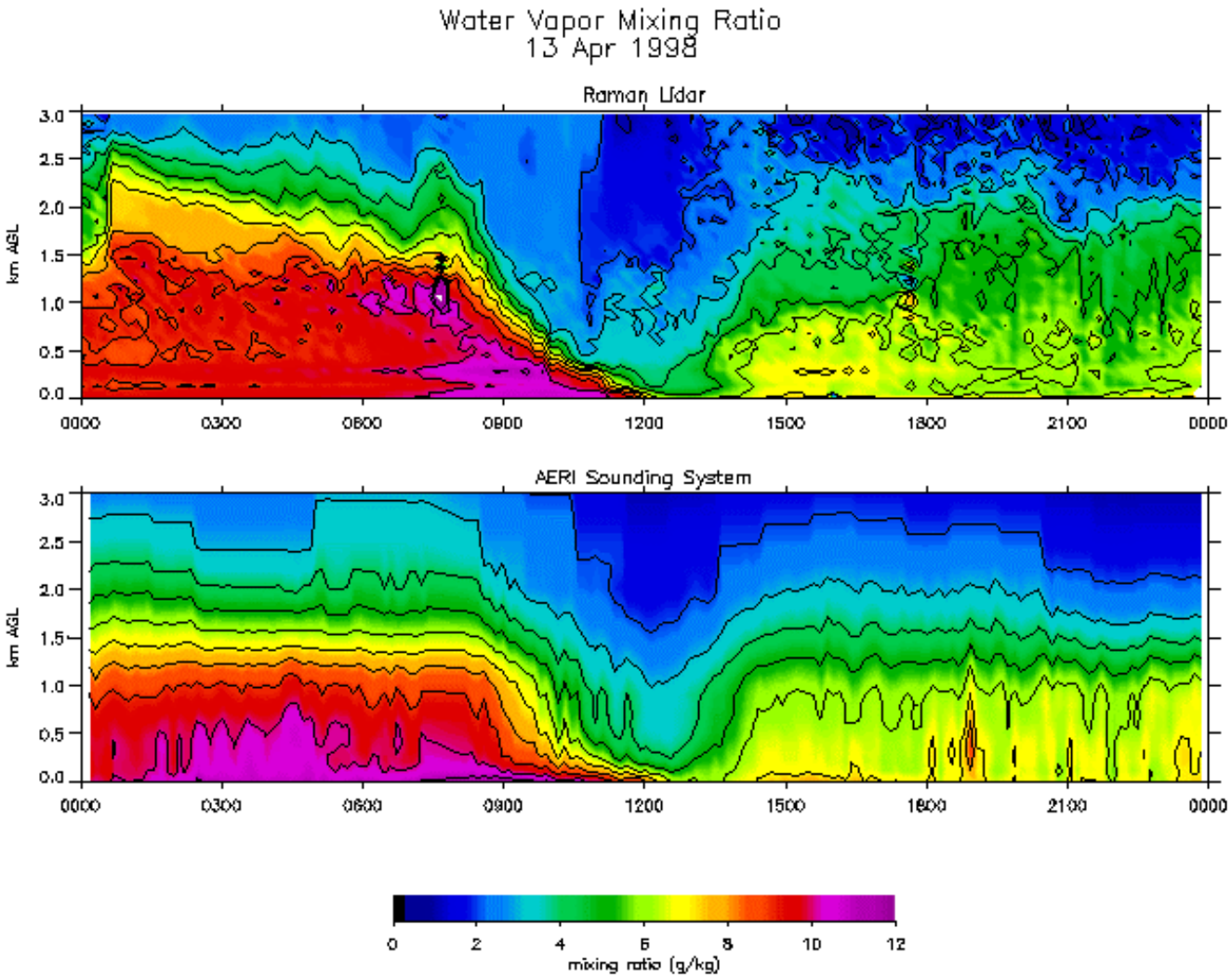

Figure 2. Time-height cross sections of water vapor mixing ratio from the Raman Lidar and AERI retrievals as a dryline passed over the SGP CART site.

By selecting coincident clear-sky samples, statistics were generated that compare one measurement technique to another. Figures 3 through 5 show the bias and root mean square (rms) between the three profiling techniques. Since diurnal calibration characteristics have been reported for radiosondes (Turner et al. 1998) and the lidar's profiles could contain a diurnal characteristic (Turner and Goldsmith 1999), these results were separated into nighttime (dotted line) and daytime cases (solid line).

The AERI-sonde comparisons show a fairly consistent bias, with the sonde about 5% to 8% dry relative to the AERI. About the same level of disagreement exists between the lidar and the sondes at night, but the differences increase to about 10% during the day, whereas the AERI-sonde residuals show no diurnal characteristic. The lidar-AERI residuals show excellent agreement at night, with differences less than 5% at night, but again the differences increase during the day. The comparisons between the

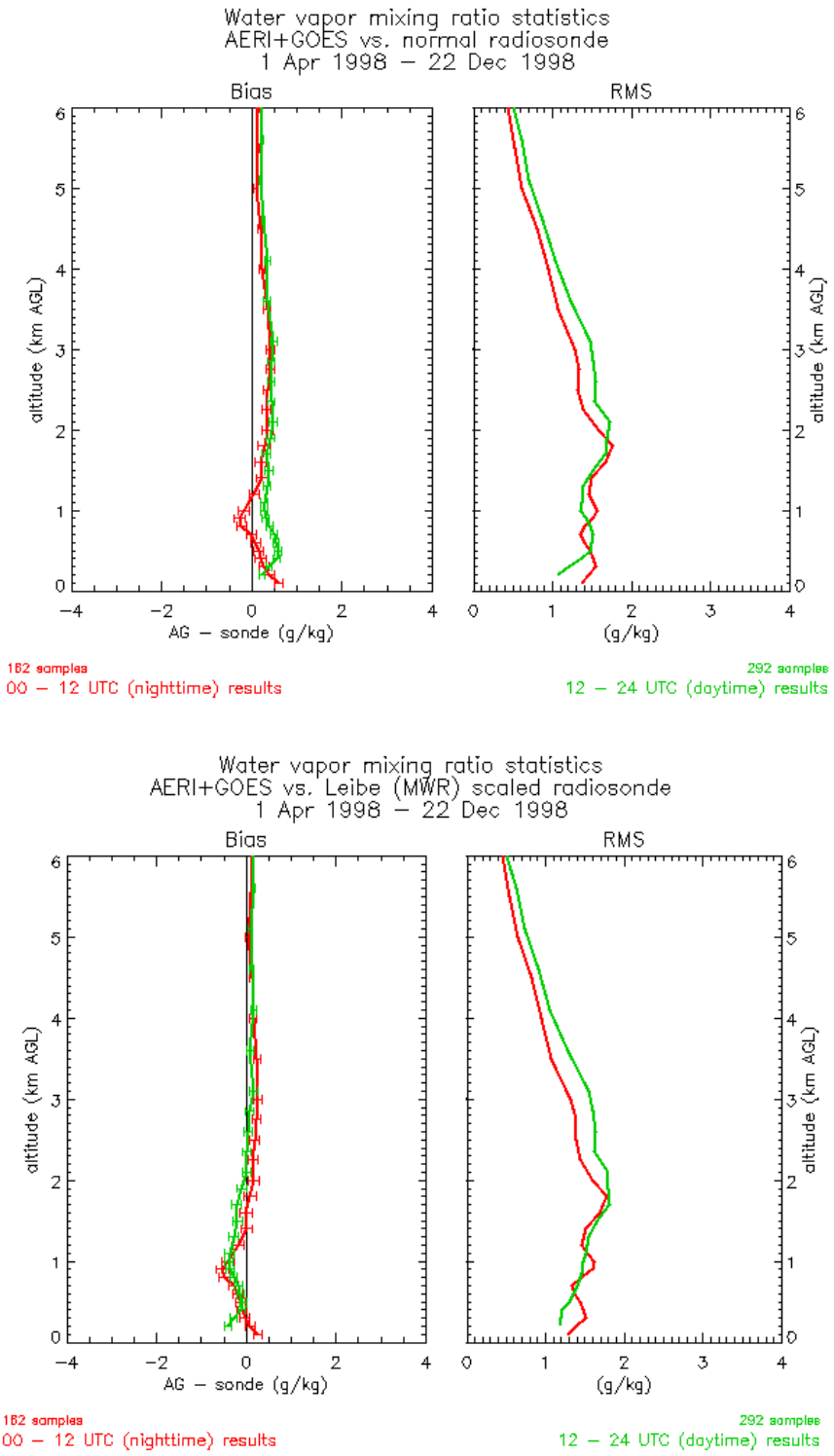

Figure 3. Mean bias and rms between the AERI+GOES and normal radiosondes (top) and MWR scaled radiosondes (bottom). The red curves are nighttime data (0 UTC to 12 UTC), which the green are daytime data (12 UTC to 24 UTC).

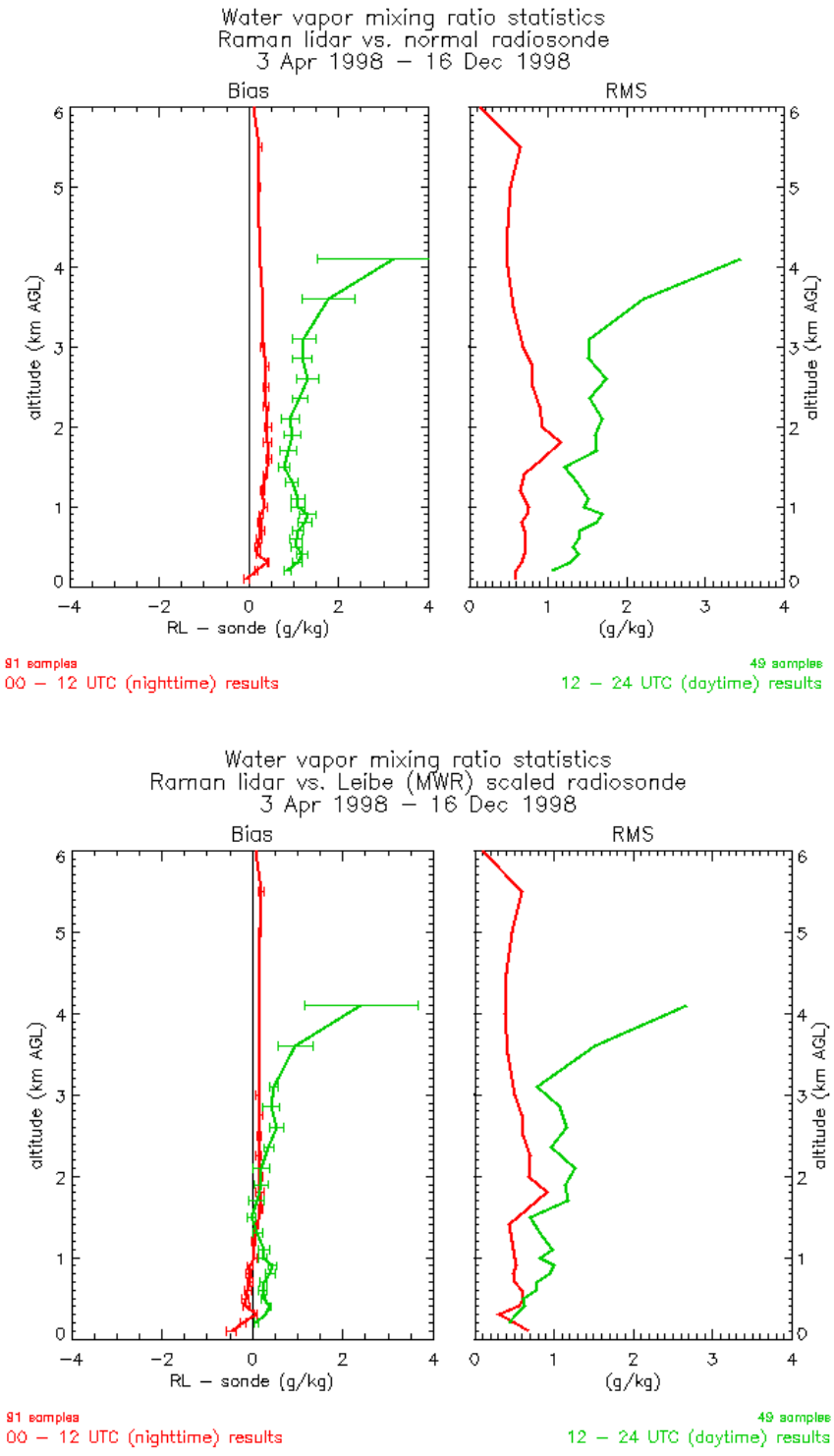

Figure 4. Mean bias and rms between the Raman Lidar and normal radiosondes (top) and MWR scaled radiosondes (bottom).

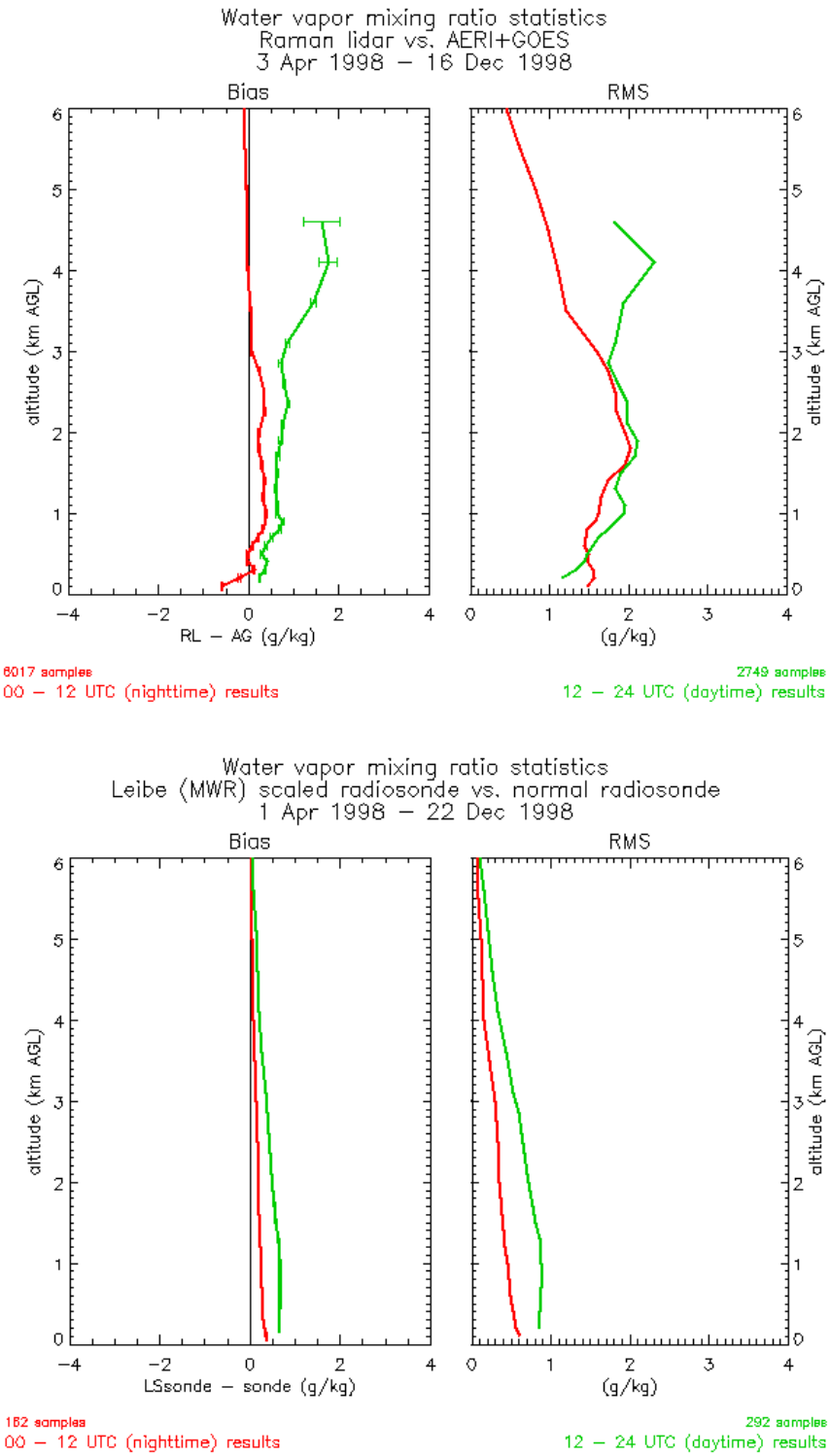

Figure 5. Mean bias and rms between the Raman Lidar and AERI retrievals (top), and MWR scaled radiosondes to the normal radiosondes (bottom).

normal and MWR scaled radiosondes on the right in Figure 5 show about a 4% to 5% difference between day and night. While more work is required in order to understand these diurnal differences, the general agreement between the three different measurement systems yields confidence in each separate measurement technique, each of which is based on complete separate physical principles.

References

Feltz, W. F., W. L. Smith, R. O. Knuteson, H. E. Revercomb, H. M. Woolf, and H. B. Howell, 1998: Meteorological applications of temperature and water vapor retrievals from the ground-based atmospheric emitted radiance interferometer (AERI). *J. Appl. Meteor.*, **37**, 857-875.

Goldsmith, J. E. M., F. H. Blair, S. E. Bisson, and D. D. Turner, 1998: Turn-key Raman Lidar for profiling atmospheric water vapor, clouds, and aerosols. *Appl. Opt.*, **37**, 4979-4990.

Melfi, S. H., D. N. Whiteman, and R. A. Ferrare, 1989: Observation of atmospheric fronts using Raman Lidar moisture measurements. *J. Appl. Meteor.*, **28**, 789-806.

Menzel, W. P., F. C. Holt, T. J. Schmidt, R. M. Aune, A. J. Schreiner, G. S. Wade, and D. G. Gray, 1998: Application of GOES-8/9 soundings to weather forecasting and nowcasting. *Bull. Amer. Metero. Soc.*, **79**, 2059-2077.

Revercomb, H. E, et al., 1993: Atmospheric Emitted Radiance Interferometer (AERI) for ARM. Preprints. *Fourth Symp. On Global Climate Change Studies*, Anaheim, California, Amer. Meteor. Soc., 46-49.

Smith, W. L, W. F. Feltz, R. O. Knuteson, H. E. Revercomb, H. B. Howell, and H. M. Woolf, 1999: The retrieval of planetary boundary layer structure using ground-based infrared spectral radiance measurements. *J. Atmos. Oceanic Technol.* In press.

Turner, D. D., and J. E. M. Goldsmith, 1999: 24-hour Raman Lidar measurements during the Atmospheric Radiation Measurement Program's 1996 and 1997 water vapor intensive observation periods. *J. Atmos. Oceanic Technol.* In press.

Turner, D. D., T. R. Shippert, P. D. Brown, S. A. Clough, R. O. Knuteson, H. E. Revercomb, and W. L. Smith, 1998: Long-term analyses of observed and line-by-line calculations of longwave surface spectral radiance and the effect of scaling the water vapor profile. In *Proceedings of the Eighth Atmospheric Radiation Measurement (ARM) Science Team Meeting*, DOE/ER-0738. U.S. Department of Energy, Washington, D.C.